Published in final edited form as:
Neuroscience. 2012 January 27; 202: 77–86. doi:10.1016/j.neuroscience.2011.11.055.

Reduction of VAMP2 Expression leads to a Kindling-Resistant Phenotype in a Murine Model of Epilepsy

Elena A. Matveeva[1], **David A. Price**[2], **Sidney W. Whiteheart**[1], **Thomas C. Vanaman**[1], **Greg A. Gerhardt**[2], and **John T. Slevin**[3,4]

[1]Department of Molecular & Cellular Biochemistry, University of Kentucky Medical Center

[2]Department of Anatomy & Neurobiology, University of Kentucky Medical Center

[3]Neurology Service Veterans Affairs Medical Center, Lexington, KY

[4]Departments of Neurology and Molecular & Biomedical Pharmacology, University of Kentucky Medical Center

Abstract

Our previous work has correlated permanent alterations in the rat neurosecretory machinery with epileptogenesis. Such findings highlighted the need for a greater understanding of the molecular mechanisms underlying epilepsy so that novel therapeutic regimens can be designed. To this end, we examined kindling in transgenic mice with a defined reduction of a key element of the neurosecretory machinery: the v-SNARE (vesicle-bound SNAP [Soluble NSF Attachment Protein] Receptor), synaptobrevin/VAMP2. Initial analysis of biochemical markers, which previously displayed kindling-dependent alterations in rat hippocampal synaptosomes, showed similar trends in both wild-type and VAMP2$^{+/-}$ mice, demonstrating that kindled rat and mouse models are comparable. This report focuses on the effects that a ~50% reduction of synaptosomal VAMP2 has on the progression of electrical kindling and on glutamate release in hippocampal subregions. Our studies show that epileptogenesis is dramatically attenuated in VAMP2$^{+/-}$ mice, requiring both higher current and more stimulations to reach a fully kindled state (2 successive Racine stage 5 seizures). Progression through the five identifiable Racine stages was slower and more variable in the VAMP2$^{+/-}$ animals compared to the almost linear progression seen in wild-type littermates. Consistent with the expected effects of reducing a major neuronal v-SNARE, glutamate-selective, microelectrode array (MEA) measurements in specific hippocampal subregions of VAMP2$^{+/-}$ mice showed significant reductions in potassium-evoked glutamate release. Taken together these studies demonstrate that manipulating the levels of the neurosecretory machinery not only affects neurotransmitter release but also mitigates kindling-induced epileptogenesis.

Keywords

kindling; epileptogenesis; hippocampus; glutamate; SNARE

Corresponding author: John T. Slevin, MD, Neurology Service (127), Veterans Affairs Medical Center, Lexington, KY 40511, Tel: 859 218-5028, FAX: 859 281-4817, jslevin@uky.edu.

Disclosure of conflict of interest GG is the sole proprietor of Quanteon, LLC that makes the FAST 16 mKII recording system used in these studies. None of the other authors has any conflicts to disclose. We confirm that we have read the Journal's position on issues involved in ethical publication and affirm that this report is consistent with those guidelines.

Epileptogenesis is a complex process involving molecular, cellular, and neural network alterations that culminate in uncontrolled synaptic activity (Mody, 1993, McNamara, 1995, Bertram, 2007). In some respects, the process mimics the alterations occurring during the normal formation of long-term memory, including distinct changes in hippocampal mnemonic processes (Goddard et al., 1969, Hannesson and Corcoran, 2000). Understanding the molecular mechanisms that underlie epileptogenesis is paramount to devising novel, rational therapies to treat the most intransigent types of epilepsy which are difficult to control and require drastic interventional strategies. Studies from this laboratory have used the electrical kindling model, in rodents, to evaluate the possibility that altered presynaptic vesicular fusion is a potential driver of epileptogenesis. Kindling was first described by Goddard and colleagues as a process of progressive and permanent intensification of epileptiform after-discharges that culminates in generalized seizures in response to repeated subconvulsive electrical stimulation (Goddard et al., 1969). The development of kindling in rodents is characterized by clearly defined electrographic and behavioral stages (Racine, 1972), which mimic complex partial seizures (Racine stage 1–2) and secondarily generalized motor seizures (Racine stages 3–5) in humans. Once the fully kindled state is achieved, spontaneous generalized convulsions may occur throughout the lifespan of the animal.

We previously showed (Matveeva et al., 2003, Matveeva et al., 2007, 2008) that electrical kindling in rats leads to a significant, asymmetric accumulation of one component of the secretory machinery, the 7S SNARE complex (7SC). This heterotrimer complex of membrane proteins is composed of the t-SNAREs, syntaxin 1 and SNAP-25, from the active zone membrane, and the v-SNARE, synaptobrevin/VAMP2, from the synaptic vesicle membrane. It represents the minimal complex required for membrane fusion, though clearly other regulators control the efficacy of its formation (Weber et al., 1998, Jahn and Scheller, 2006). Our work has also detected both transient and permanent changes in the levels of proteins that regulate SNARE complex assembly. Of the eight regulators examined (α-SNAP, NSF, SV2A/B, Munc18a/nSec1, Munc13-1, complexin 1, 2, and synaptotagmin I), only SV2 and NSF showed significant long-term alterations in the hippocampus following kindling (Matveeva et al., 2008). These changes are independent of the stimulation site (*i.e.*, entorhinal cortex, amygdalar, septal kindling) and are specific to the ipsilateral hippocampus, occurring only in CA1 and dentate gyrus (DG) subregions (Matveeva et al., 2007). No changes have been observed in other limbic areas (*e.g.*, olfactory bulb) or in non-limbic regions (*e.g.* cerebellar cortex, occipital or frontal cortex; (Matveeva et al., 2003). Taken as a whole, our studies indicate that alterations in the machinery required for neurotransmitter release, at the very least, correlate with stages of epileptogenesis. What remains is to determine if these changes are causative.

In the present manuscript, we extend our studies to genetically-altered mice that express lower levels of the key element of the secretory machinery: the v-SNARE, synaptobrevin/VAMP2. VAMP2, while not the only neuronal v-SNARE, is the dominant one responsible for the bulk of neurotransmission (Schoch et al., 2001). Neurons from mice lacking VAMP2 show a ~90% decrease in neurotransmitter release. $VAMP2^{-/-}$ pups are not viable *ex utero* due to an inability to breath. Although viable, mice with a single VAMP2 gene ($VAMP2^{+/-}$) express only ~50% of the VAMP2 levels seen in wild-type, $VAMP2^{+/+}$ controls. We report that $VAMP2^{+/-}$ mice also show up to a 50% reduction in the peak amplitude of both resting and evoked glutamate release in CA1, CA3 and DG of the hippocampal formation. Most importantly, the $VAMP2^{+/-}$ mice are substantially more resistant to electrical kindling than wild-type animals, requiring on average 1.5 times the after discharge (AD) kindling current and more than 2.5 times the number of stimulations to reach a fully kindled state (operationally defined here as 2 successive Racine stage 5 seizures). Our studies

demonstrate that epileptogenesis can be altered by modulating the activities of specific elements of the neurosecretory machinery. This mechanistic insight should help in developing novel anti-epileptic therapeutics.

2 Experimental Procedures

2.1 Preparation of Kindled and Control Animals and Tissues

2.1.1 Mouse Strains—The C57Bl/6-VAMP2$^{+/-}$ mice were a generous gift from Dr. Thomas Sudhof, (University of Texas, Southwestern) and were bred, maintained, and used according to a University of Kentucky IACUC approved protocol. The genotype of each animal used was determined by PCR using DNA prepared from tail biopsies according to Schoch *et al*.(Schoch et al., 2001).

2.1.2. Surgical Preparation—Surgery was performed in a David Kopf stereotaxic apparatus fitted with a mouse adapter after induction of anesthesia with 2-3% isoflurane; at the conclusion, animals were allowed to recover for 10-14 days prior to initiation of kindling. Teflon-coated, stainless steel bipolar twisted electrodes were implanted in the right amygdala using coordinates based on bregma (AP: -1.5; ML: +3.5; DV: -4.6) and adapted from Paxinos & Franklin (Paxinos and Franklin, 2003). Kindled and surgical-control mice were treated identically. To assess electrode placement, a random sampling from each group of treated animals was processed for histological analysis. Aspects of the surgery have been previously described (Slevin and Ferrara, 1985, Matveeva et al., 2007).

2.1.3. Kindling Techniques—Animals were tested for their AD threshold prior to kindling: a Grass S88 stimulator delivered a 1 sec train of biphasic square wave pulses (1 msec pulse duration, 60 Hz) starting at an initial 100 μA until an AD was recorded on an electroencephalogram (EEG). This AD threshold was used for subsequent stimulation. The entire experimental apparatus used has been described (Matveeva et al., 2003). AD threshold stimuli were administered once/day, five days/week until an animal experienced two consecutive Racine Stage 5 seizures consisting of tonic-clonic activity with loss of postural control/falling (Racine, 1972). No animals experienced a spontaneous generalized seizure within at least 1 week prior to euthanatization as verified by daily inspection of cages for evidence of excessive defecation, blood, or other signs of bodily injury and by direct visual and auditory scrutiny for up to 1 hr daily. Animals did not undergo continuous split screen video electroencephalographic (SSV-EEG) surveillance during this time, so it is possible a seizure may have gone undetected. However, we have previously demonstrated that a generalized seizure *per se* does not affect the 7SC ratio in the rat (Matveeva et al., 2003).

2.2 Analysis of 7S SNARE Complexes (7SC) and SNARE Regulators

Animals were euthanatized by decapitation following a 30 day latent period after experiencing 2 consecutive Stage 5 seizures, their brains were rapidly removed and the hippocampi excised on ice. Percoll-gradient-purified synaptosomes were prepared from individual hippocampi as previously described (Dunkley et al., 1986, Dunkley et al., 1988). Extracts were prepared by incubating equal quantities of synaptosomal protein in sodium dodecyl sulfate polyacrylamide gel electrophoresis (SDS–PAGE) sample buffer for 30 min at 37°C (see Figure 1). Under these conditions, monomeric SNAREs are denatured but the thermally stable 7SC fails to disassemble (Matveeva et al., 2003). After electrophoresis and transfer to PVDF membranes (Millipore), these complexes were probed by western blotting using antibodies against the t-SNARE, syntaxin 1 (HCP-1; (Inoue and Akagawa, 1992) as previously described (Matveeva et al., 2003). Western-blot-based detection of 7SC was performed using alkaline phosphatase-coupled secondary antibodies with Vistra ECF™ for visualization and images were obtained using a Typhoon 9400 imager (GE Healthcare Bio-

Sciences, Piscataway, NJ). The raw data were the integrated fluorescence intensities for all pixels in a given immuno-decorated protein band as determined by ImageQuant 5.2 software (GE Healthcare Bio-Sciences, Piscataway, NJ) in arbitrary units. This method is quantitative over at least two orders of magnitude. Subsaturating levels of protein are loaded onto the gels but saturation of the western blot signals was still monitored using the ImageQuant software. To normalize for protein loading, the fluorescence intensity of all 7SC bands (see Figure 1) was standardized to the intensity of the syntaxin 1 monomer, which we have shown to be unchanged on kindling by comparison to immune-detected actin monomer (data not shown, and see Figure 1).

Analysis of other secretory machinery proteins was performed by western blotting using the methods above. NSF was detected with the 2E5 monoclonal antibody (Tagaya et al., 1993, Whiteheart et al., 1994). Tomosyn was detected with an antibody from BD Biosciences (San Jose, CA, USA). Anti-VAMP2 monoclonal antibody (C1 69.1) was a generous gift from Dr. R Jahn, (Max Planck Institute, Gottingen, Germany). The monoclonal antibody to SV2 (which detects both A and B isoforms) was obtained from the Developmental Studies Hybridoma Bank developed under the auspices of the NICHD and maintained by the University of Iowa, Department of Biological Sciences, (Iowa City, IA). Fluorescence intensities of the bands in each lane were normalized to the intensity of the syntaxin 1 band in the same lane. To standardize measurements taken on different days, the syntaxin 1-normalized, average fluorescence intensity of an immuno-decorated protein from the hippocampi of naive controls (in a gel set) was used. To determine “Total Relative Value”, normalized ipsilateral and contralateral measurements from either experimental or control animals were summed, divided by two, and compared to the averaged surgical control (Total Value = [(Contralateral/Syntaxin 1 + Ipsilateral/ Syntaxin 1)/2] /[$\text{Contralateral}_{\text{control}}$/ Syntaxin 1]). If no changes in protein level occur, then the ratio should be unity.

2.3 In Vivo Glutamate Release Measurements

Enzyme-based, microelectrode arrays (MEA) were used to measure glutamate *in vivo*. Acute non-survival recordings (under constant isoflurane anesthesia) were performed as described by Hascup *et al*. (Hascup et al., 2011), see below.

2.3.1 Microelectrode Array (MEA) Preparation—Glutamate oxidase (GluOX) was used to catalyze the breakdown of glutamate into the reporter molecule, hydrogen peroxide, which can be oxidized by the MEA. The MEA consisted of four platinum recording sites, 15 × 333 μm, arranged in dual pairs which allows self-referencing for more selective glutamate measures as described (Burmeister and Gerhardt, 2001, Day et al., 2006). One pair of recording sites was configured for glutamate measures, while the other pair was configured to measure background currents that can be subtracted. A 10 μL solution of 1% bovine serum albumin (BSA), 0.125% glutaraldehyde, and 1% GluOX was prepared, and a dissecting microscope and microsyringe were used to manually apply a small drop (~0.1 μL) of the enzyme solution onto the lower pair of platinum recording sites. The same procedure was used to coat the top pair of platinum recording sites with a solution containing 1% BSA and 0.125% glutaraldehyde. After coating, the MEAs were cured for at least 48 hours in a low humidity environment. A size exclusion layer of 1,3-phenylenediamine (mPD) was electroplated on the recording sites to increase the selectivity for glutamate. (This size exclusion layer allows passage of small molecules such as hydrogen peroxide, but prevents the passage of large molecules such as ascorbic acid and dopamine from reaching the platinum recording sites). A 5 mM mPD solution was prepared in deoxygenated PBS. The MEA was connected to the FAST-16 MKII system (Fast Analytical Sensing Technology Mark II, Quanteon, L.L.C.) and the tip of the MEA placed in the mPD solution. The electroplating tool applied a potential as a triangular wave with an offset of -0.5 V, peak to

peak amplitude of 0.25 V at a frequency of 0.05 Hz for 20 minutes to electroplate the mPD on the platinum recording sites.

A pre-pulled single-barrel micropipette (1 mm o.d., 0.58 mm i.d. glass, A-M Systems Inc., Everett, WA) was attached to each ceramic microelectrode with Sticky Wax (Kerr Lab Corporation, Orange, CA), which allowed for the intracranial application of a KCl solution (70 mM KCl, 79 mM NaCl, 2.5 mM $CaCl_2$, pH 7.4) to study stimulus-evoked glutamate release. The tips of the micropipettes were typically pulled to an inner diameter of 10 μm, and positioned 50-75 μm away from the microelectrode surface, centered in the 100 μm space between the dorsal and ventral platinum recording pairs.

2.3.2 MEA Placement—Deep brain structure recordings were taken from the DG (AP: -2.3, ML: +/- 1.0, DV: - 2.1); CA3 (AP: -2.3, ML: +/- 2.7, DV: -2.0); and CA1 (AP: -2.3, ML: +/- 1.5, DV: -1.4). Coordinates for implantation were calculated from bregma and based on those of Paxinos and Franklin (Paxinos and Franklin, 2003). The DV coordinate was taken relative to the surface of the brain. To confirm correct placement of the MEA, green dye was applied locally via pressure ejection and 30 μm coronal cryosections were stained with Cresyl violet following *in vivo* electrochemical recordings as shown in Figure 4.

2.3.3 In Vivo Anesthetized Recording—Mice were anesthetized with 2-3% isoflurane, placed in a stereotaxic frame, and body temperature was maintained at 37°C with a water pad connected to a recirculating water bath (Gaymar). A craniotomy was performed and the overlying dura was removed to provide access to the DG, CA3 and CA1 hippocampal subregions. A miniature Ag/AgCl reference was implanted into the superficial cortex at a remote site from the recording areas. The attached micropipette was filled with isotonic KCl (70 mM KCl, 79 mM NaCl, 2.5 mM $CaCl_2$); all solutions were filtered using a sterile filter (0.20 μm) with a pH 7.4. The micropipette was attached with tubing to a Picospritzer III to control ejection volume, with the use of a stereomicroscope fitted with a reticule to monitor volume displacement (Friedemann and Gerhardt, 1992).

2.4 Data Analyses

The ipsilateral/contralateral 7SC band intensity ratios and quantified secretory machinery proteins determined from hippocampi of chronically kindled (≥ 1 month) and naïve $VAMP2^{+/+}$ controls were analyzed by ANOVA and *post hoc* t-tests using Fisher's protected least significant differences procedure, as more fully described previously (Matveeva et al., 2007, 2008). AD thresholds and number of stimulations for $VAMP2^{+/+}$ (WT) and $VAMP2^{+/-}$ mice were each analyzed by Student's unpaired t-tests. Amperometric data and event markers were analyzed using custom exported Excel ™ - based software (Quanteon LLC, Lexington, KY) to determine KCl-induced maximum amplitude and peak area phasic glutamate release. For tonic levels, a 10 sec average was taken after the electrode reached a stable baseline for at least 20 min, then the background current from the sentinel site was subtracted from the current of the GluOX site for a more selective glutamate measure. Because we were interested in determining a difference between naïve (non-stimulated) WT and $VAMP2^{+/-}$ genotypes within a single hippocampal region, glutamate electrochemical metrics (glutamate levels, peak amplitudes and peak areas), were analyzed by Student's unpaired t-tests. We have performed this type analysis previously as more fully described in (Stephens et al., 2009).

3. Results

3.1 Alterations in the Secretory Machinery in Kindled Mice

We previously showed reproducible, stage- and region-specific differences in the levels of certain elements of the secretory machinery in kindled *vs*. control rats. The relative levels of 7SC are asymmetrically increased in the ipsilateral hippocampi of fully kindled rats (Matveeva et al., 2003, Matveeva et al., 2007, 2008). These studies provided strong, but indirect, support for the hypothesis that kindling results from stimulus-induced alterations in the neurosecretory machinery. The studies presented here represent our first attempt to directly assess the role of specific proteins in kindling. This has necessitated switching to the mouse model owing to the availability of transgenic animals. Figure 1 shows the analysis of various components of the secretory apparatus in hippocampal synaptosome preparations from VAMP2$^{+/-}$ and WT (VAMP2$^{+/+}$) mice as described in Methods. In Panel A, VAMP2 levels detected in samples from VAMP2$^{+/-}$ mice were ~50% of those found in WT animals (Figure 1A). Levels of other SNAREs and or SNARE regulators were unchanged. Panel B shows the immune-detection of murine 7SC by western blotting of SDS-PAGE-resolved hippocampal synaptosomes. The complexes denoted by the braces contain both t-SNAREs (detected with anti-syntaxin-1 Abs) and v-SNAREs (detected with anti-VAMP2 Abs) and were not apparent when the samples were boiled prior to analysis. For the studies presented here, all of the bands in this region of the SDS-PAGE gel were considered 7SC. These bands were detected and quantified using the anti-syntaxin-1 antibody and normalized to the level of syntaxin-1 monomer. As shown in Panel C, the levels of 7SC were found to be identical in right *vs*. left hippocampal synaptosomes from naïve WT animals. The level of monomer was constant as compared to actin controls also shown.

We first sought to determine if the kindling-induced 7SC asymmetry, previously demonstrated in rat hippocampal synaptosomes, occurs in kindled mice. To accomplish this, we examined the ratios of 7SC in synaptosomes from the ipsilateral and contralateral hippocampi. In Figure 2A, untreated mice (Naïve) had the expected ipsilateral/contralateral ratio of one. Following a 30-day latent period subsequent to experiencing 2 consecutive Stage 5 kindled seizures, both the WT (VAMP2$^{+/+}$) and VAMP2$^{+/-}$ mice showed a ratio greater than one. This indicates that 7SC accumulation in mice was asymmetrically enriched in the hippocampus ipsilateral to the stimulation site and was not an acute effect of a generalized seizure. We next examined both genotypes to determine if kindling-dependent alterations in SV2 (black bars), NSF (white bars), and tomosyn (gray bars) occur in mice as they do in rats. As seen in Figure 2B, there was a modest increase in SV2 in synaptosomal preparations from hippocampi of fully kindled WT (VAMP2$^{+/+}$) and VAMP2$^{+/-}$ mice similar to what we have observed in rats (Matveeva et al., 2007, 2008). Interestingly, the levels of SV2 in the hippocampi of kindled VAMP2$^{+/-}$ mice (1.12 ± 0.04, n=9) increased by less than that observed in hippocampi from WT mice (1.30 ± 0.04, n=6). Tomosyn levels (gray) were not altered 30 days after cessation of kindling stimuli. This was also seen in rats: tomosyn levels were only transiently elevated early in the process of kindling and then returned to normal levels with persistence through a 30 day latent period (Matveeva et al., 2008). The levels of NSF (white) were not significantly altered by kindling in either strain. Amygdala kindled rats show a trend toward decreasing NSF after a 30-day latent period following two stimulus-induced Stage 5 seizures (Matveeva et al., 2007) that becomes significant after a 12 month latency in those animals that maintain 7SC asymmetry (Matveeva et al., 2008). Taken together, these data indicate that the murine amygdala-kindled model recapitulates most of the molecular features that we have observed in the rat amygdala kindling model.

3.2 Effect of VAMP2 Reduction on Kindling-Induced Epileptogenesis

To probe the roles of the presynaptic neurosecretory machinery in epileptogenesis, we chose to manipulate the VAMP2 gene because its protein product is central to 7SC formation and to neurotransmitter release. As noted above, the levels of VAMP2 found in the $VAMP2^{+/-}$ mice were ~50% of those found in their WT littermates. Figure 3 shows that the $VAMP2^{+/-}$ mice were substantially resistant to kindling, compared to WT littermates. They had a higher initial AD threshold and required more stimulations to reach two successive stage 5 seizures. The average initial AD threshold subsequently used during the course of kindling for the cohort of $VAMP2^{+/-}$ mice (646 μA ± 48, n=13) was significantly ($P<0.0002$, Student's t-test) higher than for the WT mice (397 μA ± 36, n=16). It should be noted that for all animals the initial AD current was determined by starting at low amperages (100 μA) and ramping up by 100 μA increments until an AD was detected. The difference observed between cohorts represents the minimal current necessary to achieve an AD. While there was some variation from animal to animal in both cohorts, the differences between WT and $VAMP2^{+/-}$ mice were clearly significant.

An even greater difference ($P<0.0004$, Student's t-test) was observed when the number of stimulations required for full kindling were compared (Figure 3B). The $VAMP2^{+/-}$ animals, despite having a higher average stimulating current applied, required nearly three times as many stimulations (19.6 ± 2.3, n=13) as WT mice (7.4 ± 0.6, n=16). The progression through the various kindling behavioral stages suggests another interesting phenomenon. As illustrated in Figure 3C, WT animals showed a steady, almost linear progression from stage 1 to 5, achieving 2 consecutive Stage 5 seizures on average by day 7. As in rats, little deviation from this linear pattern occurred, once evidence of electrographic and behavioral progression was detected. In contrast, there were substantial oscillations in the progression of the $VAMP2^{+/-}$ mice (Figure 3D) despite their higher initial AD threshold, which current was used for subsequent stimulations until two stage 5 seizures were provoked. On average the progression through each kindling stage was clearly slower, requiring a greater number of stimulations to reach each stage. The slowest WT mouse to kindle required 13 stimulations; only 3 (of 13) $VAMP2^{+/-}$ animals experienced 2 consecutive Stage 5 seizures in fewer than 13 days. Strikingly, most $VAMP2^{+/-}$ animals showed an inability to maintain a kindling stage, reverting to lower stages throughout the process. This phenomenon was seen in only one of 16 WT animals. Hence, ~80% of VAMP2 deficient animals were not fully kindled after 14 days of stimulation; on average they required 17-18 days of stimulation to achieve 2 consecutive Stage 5 seizures. It is highly unlikely that this difference in phenotype between WT and $VAMP2^{+/-}$ mice is due to electrode placement, as equivalent electrode placement surgeries and coordinates were used and the potential for misplacement is equal for both strains. The molecular basis for this instability of kindling progression is unclear but is clearly related to the reduction in VAMP2 levels.

3.3 Functional Correlates of VAMP2 Deficiency

The above studies demonstrate that altering the levels of VAMP2 affects kindling. Equally important is to demonstrate that altering VAMP2 expression affects neurotransmitter release. Based on previous studies of cultured neurons from $VAMP2^{-/-}$ pups (Schoch et al., 2001), one would predict that a reduction in this central v-SNARE would negatively affect neurotransmitter release, but this had not been demonstrated *in vivo*. Since enhanced hippocampal glutamate release is a primary consequence of kindling induced by stimulation from several sites and may be integral to epileptogenesis (Geula et al., 1988, Jarvie et al., 1990, Kamphuis et al., 1991, Minamoto et al., 1992, Yamagata et al., 1995, Ueda et al., 2000), we examined the effects of decreased VAMP2 on glutamate release in the hippocampus, *in situ* in kindled mice. Advances in MEA technologies have provided the tools necessary to monitor excitatory neurotransmitter (*i.e.*, glutamate) release *in vivo* in

localized brain regions (Hascup et al., 2011). We utilized these techniques to determine whether altered VAMP2 levels commensurately alter tonic (resting) and/or phasic (KCl-stimulated) glutamate release in specific hippocampal subregions (see Figure 4A and B for electrode placements). Illustrated in Figure 4C, there was a modest but consistent reduction of the average resting glutamate levels in the DG, CA3 and CA1 regions of VAMP2$^{+/-}$ animals. These differences were greatly amplified by the application of KCl. Figures 4D and 4E show that both the peak amplitude of response and the total amount of glutamate released, assessed as peak area, were up to two-fold higher in WT mice, particularly in CA3 and CA1. This is in direct accordance with the reduction in VAMP2 expression seen in the VAMP2$^{+/-}$ animals. These data demonstrate that diminished hippocampal VAMP2 is indeed associated with reduced hippocampal neuronal glutamate release. These data serve as an important demonstration that the VAMP2$^{+/-}$ mouse model indeed behaves as expected based on the *in vitro* analysis of cultured neurons.

4. Discussion

Our previous studies (Matveeva et al., 2003, Matveeva et al., 2007, 2008) in the rat model provide substantial, correlative evidence that alterations in specific proteins of the neurosecretory system occur during kindling. These changes are specific to discrete regions of the limbic system and accompany alterations in both behavioral/electroencephalographic profiles and glutamate release. However, the lack of pharmacological agents that directly affect the actions of these proteins as well as limited knowledge about their exact roles has made it difficult to obtain direct evidence of their specific involvement in epileptogenesis. The studies presented here are the first to provide direct evidence for the involvement of a specific neurosecretory machinery protein in kindling evolution. The fact that decreased expression of VAMP2 led to such a dramatic alteration in the course of kindling gives ample evidence of the power of this approach for future mechanistic studies of epileptogenesis.

The most striking effects observed were those on the behavioral progression of kindling. The VAMP2$^{+/-}$ mice required both higher initial AD thresholds and greater numbers of stimulations to attain the fully kindled state. An even greater delineator of the phenotypic difference was the highly erratic progression of VAMP2$^{+/-}$ animals compared to the almost predictable, consistent progression of WT animals. Racine and colleagues developed two strains of rats, *Fast* and *Slow*, based on their rate of amygdala kindling, after 6 generations of selection from an original parent population of a Long Evans Hooded and Wistar cross (Racine *et al*., 1999). Recent evidence suggests the phenotypic variance between *Fast* and *Slow* kindlers is due to a differential expression of genes related to fatty acid metabolism (McIntyre DM *et al*., 2007). Similar to VAMP2$^{+/-}$ mice, in addition to kindling resistance *Slow* rats also regress to milder behavioral stages one or more times during the kindling process. However, the initial AD threshold is the same for *Fast* and *Slow* kindlers, in contrast to the increased initial AD threshold of VAMP2$^{+/-}$ mice compared to WT. At this time there is no evidence that the similar epileptic phenotype of *Slow* rats and VAMP2$^{+/-}$ mice is based on a common molecular, biochemical or anatomic pathoetiology. However, one could speculate that the altered synaptic energetics in *Slow* rats could, among other mechanisms, reduce bursting of hippocampal glutamatergic neurons by retarding SNARE complex turnover.

Given our observations of attenuated, maximal KCl-stimulated hippocampal glutamate release in the VAMP2$^{+/-}$ animals, it seems possible that there is a stimulation threshold for epileptogenesis. The VAMP2$^{+/-}$ animals may be less likely to consistently surpass the threshold due to blunted glutamate release and thus kindling is variable or delayed. We previously showed, using time course analyses in rat hippocampus, that both biochemical and behavioral changes revert to the naïve state unless animals are stimulated past stage 3

(Matveeva *et al*., in press). Once an animal achieves Racine behavioral stage 4, the changes persist to one year, and may well be permanent (Matveeva *et al*., 2008). These data are consistent with the concept that there is a threshold, which must be exceeded for epileptogenesis to proceed to an enduring epileptic state. The fact that this process is reversible up to a point suggests that intervention to perturb this progression may successfully prevent, or at least delay, epileptogenesis. This perhaps explains the effects of levetiracetam in kindled rats (Matveeva *et al*., 2008). Clearly, the VAMP2$^{+/-}$ model will be a useful adjunct in future studies of potential anti-epileptogenic drugs.

The reductions in glutamate release were expected for an animal with half the normal level of VAMP2. Schoch *et al*. (2001) has previously demonstrated significant deficiencies in neurotransmitter release from cultured neurons from VAMP2$^{-/-}$ mice. Our current studies demonstrate consistent glutamate release defects *in vivo*, from VAMP2$^{+/-}$ mice, particularly in response to maximal depolarization induced by KCl. These defects are detectible in hippocampal subregions where we previously demonstrated kindling-induced alterations in secretory proteins(Matveeva *et al*., 2007, Matveeva *et al*., In press). The reduction in glutamate release may contribute to the kindling resistance phenotype seen here. Increases, in the hippocampus, of depolarization-induced (Matveeva *et al*., In press) and KCl-evoked (Geula *et al*., 1988; Jarvie *et al*., 1990; Minamoto *et al*., 1992) glutamate release have been measured in electrically-kindled rats. Enhanced depolarization-induced hippocampal glutamate release has also been reported in cocaine kindled mice (Kaminski *et al*., 2011). One can speculate that a critical component of the kindling phenomenon is dysregulation of glutamate release in specific hippocampal networks. Comparison of WT and VAMP2$^{+/-}$ mice using the MEA methodology to locally (<0.03mm^3 region, see Figure 4) apply glutamate to specific brain regions (*e.g*., in entorhinal cortex, dentate gyrus) in fully awake animals may provide a direct system to test whether repetitive glutamate administration in appropriate regions can mimic the kindling phenomenon.

In the present report, as in our previous studies of rats (Matveeva *et al*., 2008, Matveeva *et al*., In press), we detected a bilateral increase in hippocampal SV2 in mice, 30 days post amygdalar kindling. VAMP2$^{+/-}$ mice showed a less robust increase in total hippocampal SV2 compared to WT. While the actual role(s) of SV2 at the synapse is unclear, SV2A$^{-/-}$ and SV2A/B$^{-/-}$ mice exhibit severe seizures and cultured autaptic hippocampal neurons lacking both isoforms demonstrate heightened glutamatergic activity and marked attenuation of short-term synaptic depression (Janz *et al*., 1999). A scenario that could reconcile these observations would be one in which increased hippocampal SV2 is part of a compensatory response to pathologically-enhanced glutamatergic activity. Consistent with this scenario, the smaller increase in SV2, observed in VAMP2$^{+/-}$ animals, correlates with a less robust increase in glutamate release. Further, the epileptic phenotype of SV2 knockouts could be due to the absence of SV2's part in a compensatory response. SV2 is a target for the levetiracetam class of antiepileptic drugs which dampen kindling (Loscher *et al*., 1998, Klitgaard and Pitkanen, 2003, Matveeva *et al*., 2008). Levetiracetam might enhance SV2 function(s) and thus augment its role as a compensatory response to heightened glutamatergic activity. While this is clearly speculative, it does justify future interest in pursuing the role(s) of SV2 in epileptogenesis and as a target for novel antiepileptogenic drugs.

Finally, the studies presented here show the efficacy of using MEAs and transgenic mice to examine the roles of specific elements of the neurosecretory apparatus. This approach allows the analysis of the direct effects of a specific protein on *in vivo* neurotransmitter release and on epileptogenesis. Our preliminary characterization of tomosyn$^{-/-}$ mice shows an opposite kindling phenotype to the VAMP2$^{+/-}$ mice, namely there is a dramatic enhancement of the kindling response (data not shown). Given tomosyn's purported role as a negative regulator

of SNARE complex formation (Sakisaka *et al*., 2008), these data underline the importance that uncontrolled glutamate release may have on epileptogenesis. We are actively pursuing these studies with other mutant mouse strains to define the molecular processes that beget epilepsy in hopes of elucidating potential targets for therapeutic intervention and possible strategies to disrupt the epileptogenic process.

Acknowledgments

We acknowledge the technical assistance of Ramona Alcala and Verda A. Davis. This work is supported by the Department of Veterans Affairs (JTS), a grant from DARPA (N66001-09-C-2080) (GG), and HL56652 and HL091893 (SWW).

References

Bertram E. The relevance of kindling for human epilepsy. Epilepsia. 2007; 48(Suppl 2):65–74. [PubMed: 17571354]

Burmeister JJ, Gerhardt GA. Self-referencing ceramic-based multisite microelectrodes for the detection and elimination of interferences from the measurement of L-glutamate and other analytes. Analytical chemistry. 2001; 73:1037–1042. [PubMed: 11289414]

Day BK, Pomerleau F, Burmeister JJ, Huettl P, Gerhardt GA. Microelectrode array studies of basal and potassium-evoked release of L-glutamate in the anesthetized rat brain. J Neurochem. 2006; 96:1626–1635. [PubMed: 16441510]

Dunkley PR, Heath JW, Harrison SM, Jarvie PE, Glenfield PJ, Rostas JA. A rapid Percoll gradient procedure for isolation of synaptosomes directly from an S1 fraction: homogeneity and morphology of subcellular fractions. Brain Res. 1988; 441:59–71. [PubMed: 2834006]

Dunkley PR, Jarvie PE, Heath JW, Kidd GJ, Rostas JA. A rapid method for isolation of synaptosomes on Percoll gradients. Brain Res. 1986; 372:115–129. [PubMed: 3011205]

Friedemann MN, Gerhardt GA. Regional effects of aging on dopaminergic function in the Fischer-344 rat. Neurobiology of aging. 1992; 13:325–332. [PubMed: 1522947]

Geula C, Jarvie PA, Logan TC, Slevin JT. Long-term enhancement of K+-evoked release of L-glutamate in entorhinal kindled rats. Brain Res. 1988; 442:368–372. [PubMed: 3370453]

Goddard GV, McIntyre DC, Leech CK. A permanent change in brain function resulting from daily electrical stimulation. Exp Neurol. 1969; 25:295–330. [PubMed: 4981856]

Hannesson DK, Corcoran ME. The mnemonic effects of kindling. Neurosci Biobehav Rev. 2000; 24:725–751. [PubMed: 10974354]

Hascup KN, Hascup ER, Stephens ML, Glaser PE, Yoshitake T, Mathe AA, Gerhardt GA, Kehr J. Resting Glutamate Levels and Rapid Glutamate Transients in the Prefrontal Cortex of the Flinders Sensitive Line Rat: A Genetic Rodent Model of Depression. Neuropsychopharmacology. 2011

Inoue A, Akagawa K. Neuron-specific antigen HPC-1 from bovine brain reveals strong homology to epimorphin, an essential factor involved in epithelial morphogenesis: identification of a novel protein family. Biochem Biophys Res Commun. 1992; 187:1144–1150. [PubMed: 1530610]

Jahn R, Scheller RH. SNAREs - engines for membrane fusion. Nat Rev Mol Cell Biol. 2006; 7:631–643. [PubMed: 16912714]

Janz R, Goda Y, Geppert M, Missler M, Sudhof TC. SV2A and SV2B function as redundant Ca2+ regulators in neurotransmitter release. Neuron. 1999; 24:1003–1016. [PubMed: 10624962]

Jarvie PA, Logan TC, Geula C, Slevin JT. Entorhinal kindling permanently enhances Ca2(+)-dependent L-glutamate release in regio inferior of rat hippocampus. Brain Res. 1990; 508:188–193. [PubMed: 1968356]

Kamphuis W, Huisman E, Veerman MJ, Lopes da Silva FH. Development of changes in endogenous GABA release during kindling epileptogenesis in rat hippocampus. Brain Res. 1991; 545:33–40. [PubMed: 1860054]

Klitgaard H, Pitkanen A. Antiepileptogenesis, neuroprotection, and disease modification in the treatment of epilepsy: focus on levetiracetam. Epileptic Disord. 2003; 5(Suppl 1):S9–16. [PubMed: 12915336]

Loscher W, Honack D, Rundfeldt C. Antiepileptogenic effects of the novel anticonvulsant levetiracetam (ucb L059) in the kindling model of temporal lobe epilepsy. J Pharmacol Exp Ther. 1998; 284:474–479. [PubMed: 9454787]

Matveeva EA, Davis VA, Whiteheart SW, Vanaman TC, Gerhardt GA, Slevin JT. Kindling-induced asymmetric accumulation of hippocampal 7S SNARE complexes correlates with enhanced glutamate release. Epilepsia. In press.

Matveeva EA, Vanaman TC, Whiteheart SW, Slevin JT. Asymmetric accumulation of hippocampal 7S SNARE complexes occurs regardless of kindling paradigm. Epilepsy Res. 2007; 73:266–274. [PubMed: 17174072]

Matveeva EA, Vanaman TC, Whiteheart SW, Slevin JT. Levetiracetam prevents kindling-induced asymmetric accumulation of hippocampal 7S SNARE complexes. Epilepsia. 2008; 49:1749–1758. [PubMed: 18513349]

Matveeva EA, Whiteheart SW, Slevin JT. Accumulation of 7S SNARE complexes in hippocampal synaptosomes from chronically kindled rats. J Neurochem. 2003; 84:621–624. [PubMed: 12558983]

McNamara JO. Analyses of the molecular basis of kindling development. Psychiatry Clin Neurosci. 1995; 49:S175–178. [PubMed: 8612137]

Minamoto Y, Itano T, Tokuda M, Matsui H, Janjua NA, Hosokawa K, Okada Y, Murakami TH, Negi T, Hatase O. In vivo microdialysis of amino acid neurotransmitters in the hippocampus in amygdaloid kindled rat. Brain Res. 1992; 573:345–348. [PubMed: 1354551]

Mody I. The molecular basis of kindling. Brain Pathol. 1993; 3:395–403. [PubMed: 8293195]

Paxinos, G.; Franklin, KBJ. The Mouse Brain Stereotaxic Coordinates: Compact. Second Edition. New York, NY: Academic Press/Elsevier; 2003.

Racine RJ. Modification of seizure activity by electrical stimulation. II. Motor seizure. Electroencephalogr Clin Neurophysiol. 1972; 32:281–294. [PubMed: 4110397]

Sakisaka T, Yamamoto Y, Mochida S, Nakamura M, Nishikawa K, Ishizaki H, Okamoto-Tanaka M, Miyoshi J, Fujiyoshi Y, Manabe T, Takai Y. Dual inhibition of SNARE complex formation by tomosyn ensures controlled neurotransmitter release. J Cell Biol. 2008; 183:323–337. [PubMed: 18936251]

Schoch S, Deak F, Konigstorfer A, Mozhayeva M, Sara Y, Sudhof TC, Kavalali ET. SNARE function analyzed in synaptobrevin/VAMP knockout mice. Science. 2001; 294:1117–1122. [PubMed: 11691998]

Slevin JT, Ferrara LP. Lack of effect of entorhinal kindling on L-[3H]glutamic acid presynaptic uptake and postsynaptic binding in hippocampus. Exp Neurol. 1985; 89:48–58. [PubMed: 4007115]

Stephens ML, Quintero JE, Pomerleau F, Huettl P, Gerhardt GA. Age-related changes in glutamate release in the CA3 and dentate gyrus of the rat hippocampus. Neurobiology of aging. 2009

Tagaya M, Wilson DW, Brunner M, Arango N, Rothman JE. Domain structure of an N-ethylmaleimide-sensitive fusion protein involved in vesicular transport. J Biol Chem. 1993; 268:2662–2666. [PubMed: 8428942]

Ueda Y, Doi T, Tokumaru J, Mitsuyama Y, Willmore LJ. Kindling phenomena induced by the repeated short-term high potassium stimuli in the ventral hippocampus of rats: online monitoring of extracellular glutamate overflow. Exp Brain Res. 2000; 135:199–203. [PubMed: 11131504]

Weber T, Zemelman BV, McNew JA, Westermann B, Gmachl M, Parlati F, Sollner TH, Rothman JE. SNAREpins: minimal machinery for membrane fusion. Cell. 1998; 92:759–772. [PubMed: 9529252]

Whiteheart SW, Rossnagel K, Buhrow SA, Brunner M, Jaenicke R, Rothman JE. N-ethylmaleimide-sensitive fusion protein: a trimeric ATPase whose hydrolysis of ATP is required for membrane fusion. J Cell Biol. 1994; 126:945–954. [PubMed: 8051214]

Yamagata Y, Obata K, Greengard P, Czernik AJ. Increase in synapsin I phosphorylation implicates a presynaptic component in septal kindling. Neuroscience. 1995; 64:1–4. [PubMed: 7708197]

Abbreviations

7SC	7S SNARE complex
Abu	absolute units
AD	after discharge
BSA	bovine serum albumin
DG	dentate gyrus
GluOX	Glutamate oxidease
MEA	microelectrode array
mPD	1,3-phenylenediamine
NSF	N-ethylmaleimide Sensitive Factor
SDS-PAGE	sodium dodecyl sulfate–polyacrylamide gel electrophoresis
SNAP	Soluble NSF Attachment Protein
SNARE	SNAP Receptor
v (t) SNARE	vesicle-bound (target membrane) SNAP Receptor
VAMP	Vesicle Associated Membrane Protein
WT	wild-type

Highlights

- The VAMP2 SNARE was reduced by 60% in hippocampal synaptosomes of VAMP2$^{+/-}$ mice compared to VAMP2$^{+/+}$littermates.
- Amygdala kindling was attenuated in VAMP2$^{+/-}$ vs. VAMP2$^{+/+}$ mice, requiring a higher AD threshold and more stimuli.
- Progression through kindling stages oscillated in VAMP2$^{+/-}$ vs. an almost linear progression seen in VAMP2$^{+/+}$ littermates.
- 1 month post-kindling there was increased ipsilateral 7SC and bilateral SV2, greater in VAMP2$^{+/+}$ than VAMP2$^{+/-}$ hippocampus.
- 1 month post-kindling there were reductions of KCl-evoked glutamate release in VAMP2$^{+/-}$ compared to VAMP2$^{+/+}$ DG and CA3.

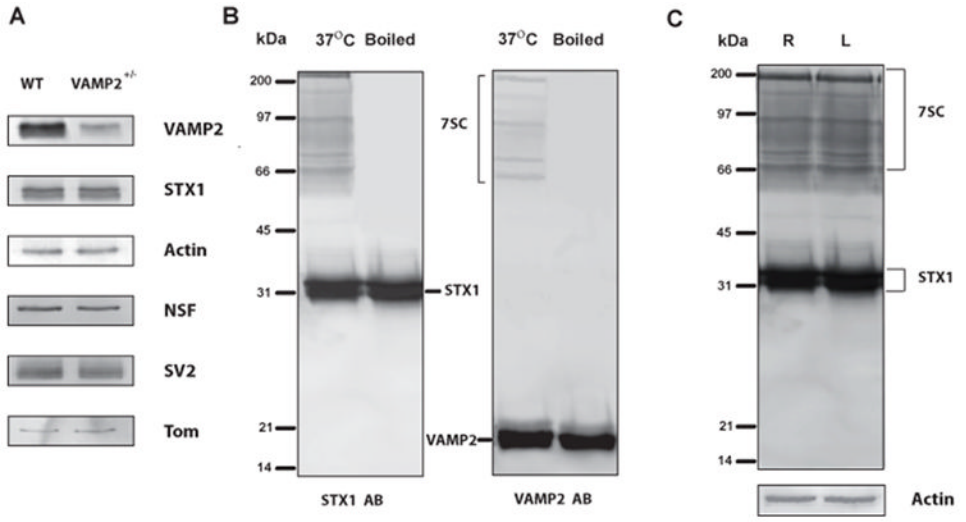

Figure 1. 7S SNARE components in hippocampal synaptosomes from WT *and* VAMP2$^{+/-}$ mice

Hippocampi were isolated from mice and synaptosomes were prepared as in Methods. ***Panel A*** shows western blot analyses for the indicated proteins. VAMP2 was decreased by ~50% in synaptosomes prepared from naive VAMP2$^{+/-}$ as compared to WT (VAMP2$^{+/+}$) mice. Other important members of the secretory apparatus in hippocampal synaptosomes: syntaxin 1 (STX1), N-ethylmaleimide Sensitive Factor (NSF), SV2, and Tomosyn (Tom) were unchanged. ***Panel B*** shows the characterization of 7S complexes from murine hippocampal synaptosomes. Synaptosomal proteins were resolved by SDS-PAGE and probed by western blotting with either anti-syntaxin1 antibody (left) or anti-VAMP2 antibody (right). The bands in the indicated range (7SC) were detected with both antibodies and disappeared upon prior boiling. These bands were considered authentic 7S complexes and were quantified as a group. ***Panel C*** illustrates the regions of the western blot that were used for 7S complex analysis. The whole region of the western blot, denoted 7SC, was quantified and normalized to the monomeric syntaxin 1 band (STX1). A ratio of the normalized ipsilateral (right hippocampus, R) and contralateral (left hippocampus, L) was used to detect asymmetric accumulation of 7SC. Actin was included as a loading control for these blots to demonstrate that monomeric syntaxin 1 also does not change and thus can be used for normalization.

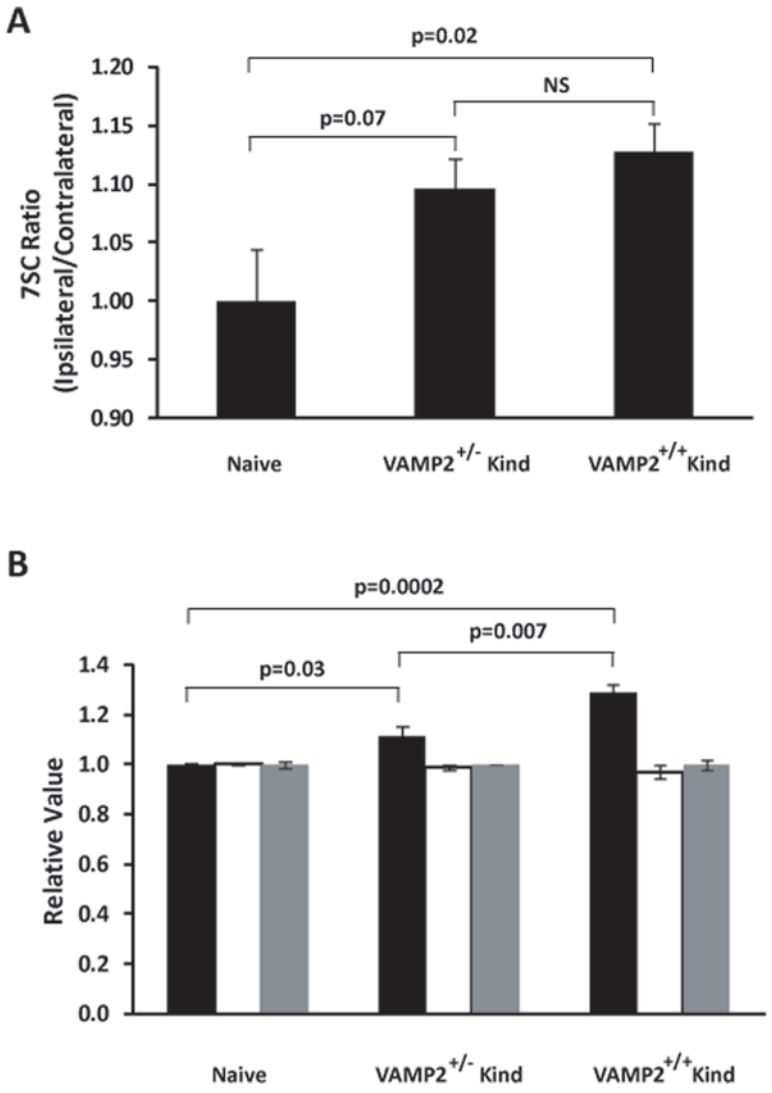

Figure 2. Analysis of the secretory apparatus in hippocampal synaptosomes from kindled mice

Hippocampi were isolated from mice euthanized after a 30 day latent period following two Racine Stage 5 seizures occurring on two consecutive days and from naïve (non-stimulated) wild-type controls; synaptosomes were prepared and 7SC was measured as in Methods and in Figure 1. ***Panel A:*** SNARE complexes were resolved by SDS-PAGE, then detected and quantified by western blot analysis as described in Methods. The graph shows the ratios of the levels of 7SC in the ipsilateral hippocampal synaptosomes compared to those in the contralateral samples; P = 0.04, single factor ANOVA; *post hoc* t-tests using Fisher's protected least significant differences procedure. P values are indicated over the relevant comparisons. Sample size (n): Naïve (5), VAMP2$^{+/-}$ (11), VAMP2$^{+/+}$ (10); error bars represent standard error of the mean (SEM). ***Panel B:*** Levels of SNARE regulators. Samples of purified synaptosomes were solubilized in SDS-PAGE sample buffer and resolved by standard SDS-PAGE. The resolved proteins were quantified as in Methods: SV2 (black bars) was increased in kindled mice: P = 0.0002 by single factor ANOVA; *post hoc* t-tests using Fisher's protected least significant differences procedure. P values are indicated over the relevant comparisons. No difference was observed in total hippocampal levels of

NSF (white bars) and tomosyn (gray bars) among groups. Sample size (n): Naïve (5), VAMP2$^{+/-}$ (9), VAMP2$^{+/+}$ (6); error bars represent SEM.

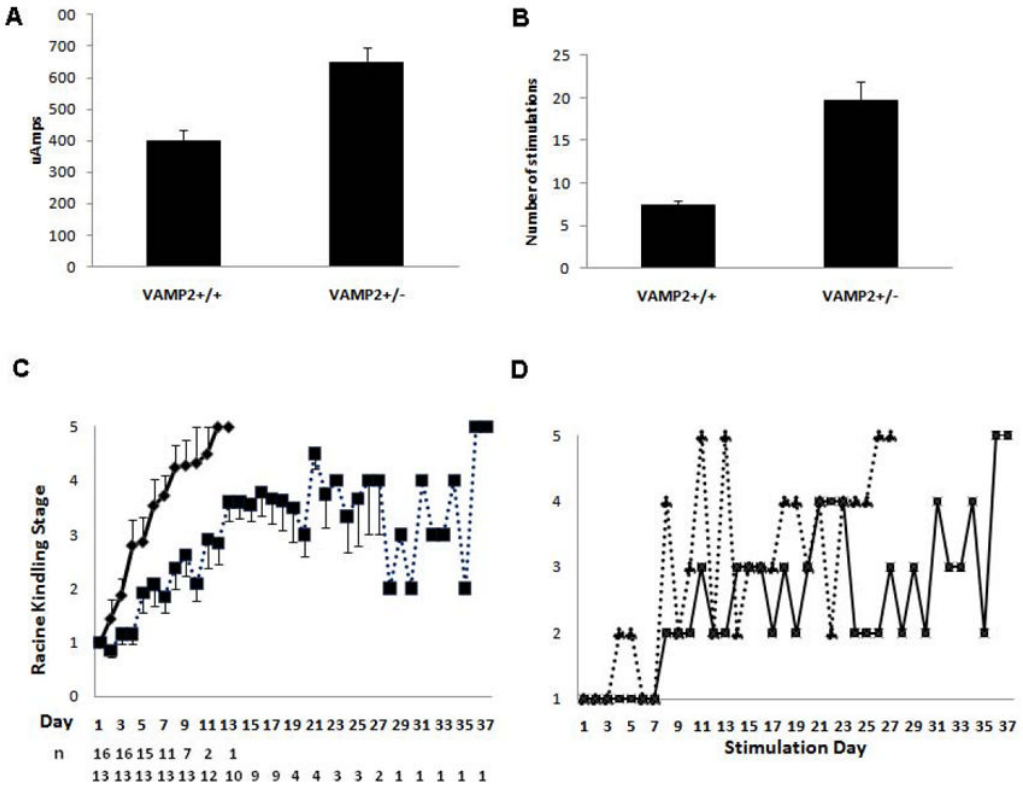

Figure 3. Kindling Parameters for Wild-Type and VAMP2$^{+/-}$ mice

Panel A: The average current required to produce an AD is different for wild-type (VAMP2$^{+/+}$) and VAMP2$^{+/-}$ mice ($P < 0.0002$, Student's t-test). These currents were used for the subsequent kindling stimulations. ***Panel B*** shows the average number stimulations (once per day) required to obtain a stage 5 seizure on 2 consecutive days. The error bars denote SEM for all animals. n=16 for VAMP2$^{+/+}$ and 13 for VAMP2$^{+/-}$ ($P < 0.0004$, Student's t-test). ***Panel C:*** Time course of kindling stage versus stimulation number (1 stimulation per day) of wild-type (VAMP2$^{+/+}$; solid line) and VAMP2$^{+/-}$ (dotted line) mice. Each point represents the mean ± SEM with n= number of animals still being stimulated at each time point. As animals achieved full kindling they were removed from the group. ***Panel D:*** The graph shows the typical unstable, oscillating course through kindling stages for two VAMP2$^{+/-}$ mice.

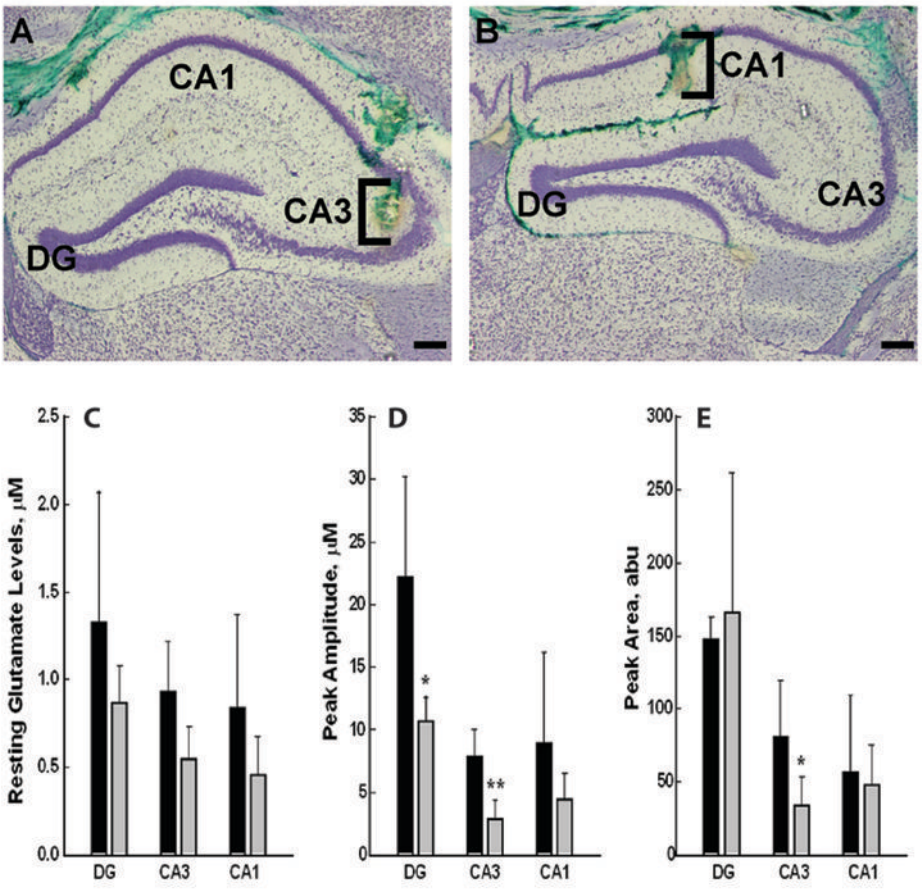

Figure 4. Resting and KCl- evoked glutamate release levels in hippocampal regions in VAMP2$^{+/+}$ and VAMP2$^{+/-}$ mice

Resting and KCl-evoked release of glutamate were determined *in vivo* in DG, CA3 and CA1 using non-kindled WT (VAMP2$^{+/+}$) and VAMP2$^{+/-}$ animals with an implanted MEA system as in Methods. ***Panels A and B:*** Electrode placement. Following electrochemical recordings, green dye was locally applied *via* pressure ejection to verify correct electrode placement. Representative micrographs of 30 μm coronal sections stained with Cresyl violet are shown; DG, CA3 and CA1 sub-regions of the hippocampus are noted. Brackets approximate the dorsal-ventral location of S2 MEA glutamate recording sites in A) CA3 and B) CA1. Scale bar = 200 μm. ***Panel C*** shows unstimulated steady state resting concentrations of glutamate. ***Panel D*** shows the peak amplitudes of KCl-evoked glutamate release in similar animals from the DG, CA3, and CA1. ***Panel E*** shows the average value for the peak areas during the full time course of recorded glutamate release. The values shown represent the averages obtained from n=3, VAMP2$^{+/+}$ and n=4, VAMP2$^{+/-}$ mice (**Panel C**) and n=5 VAMP2$^{+/+}$ and n=5 VAMP2$^{+/-}$ mice (**Panels D, E**). The error bars represent SEM, abu = absolute units; * represents $P < 0.05$, ** $P < 0.01$; Student's unpaired t-test.